 DOI: 10.1002/masy.200651212

Aerocellulose: Aerogels and Aerogel-like Materials made from Cellulose

Josef Innerlohinger, Hedda K. Weber, Gregor Kraft*

Summary: Cellulose aerogels have been prepared starting from cellulose-NMMO solutions via the classical aerogel-path. Different cellulosic materials have been tested and their influence on the properties of the product aerogels has been studied. Other parameters that have been varied include solution composition as well as the way of cellulose regeneration (solvent and temperature). More than 300 different samples were prepared and analysed. Their density is in a typical range from 0.02 g/cm^3 to 0.2 g/cm^3 and their internal surface area ranges from 100 m^2/g to 400 m^2/g. Another property investigated in detail beside density and internal surface area was the shrinkage of the cellulosic bodies during the production process.

Keywords: aerogels; biomaterials; cellulose; microstructure; *N*-methyl-morpholine-*N*-oxide (NMMO)

Introduction

Aerogels are a class of materials, which are characterised by their highly porous structure and their low solids content. They are obtained from wet gels by drying largely maintaining the openness of the structure. If the structure collapses during the drying the resulting material is termed xerogel. Although often considered a recent high-tech product, the first aerogels were actually synthesised in the 1930s by S. Kistler.[1,2] He produced a variety of aerogels from different materials like silica, alumina, rubber and even cellulose derivatives. During the last decade interest in this class of materials has re-emerged, resulting in a resurgence of scientific research dedicated to the subject.

Most commonly known are inorganic aerogels based on silica, which are already used in a couple of applications. They range from rather exotic ones like detectors for Cherenkow radiation or the capture of space dust to more common ones like sound or thermal insulation.[3] The main route for the production of organic aerogels is a sol-gel synthesis from resorcinol and formaldehyde and their derivatives.[4–6] The organic aerogels can be pyrolysed to yield aerogels consisting completely of carbon.[4,7,8] Only limited research exists in cellulose aerogels so far[9–11] although cellulose was among the first materials used to prepare aerogels as mentioned above.

Within the 6th Framework Program of the European Union the AeroCell project deals with aerogels and aerogel-like materials from cellulose.[12] The AeroCell consortium consists of ten partners from five European countries, covering both academic and industrial research. Different preparation methods for aerogels from cellulosic materials are investigated and the obtained samples are thoroughly analysed and tested for their suitability for selected applications.[13] Aerogels based on cellulose have connections to two of today's hot research topics: first, since they are made from a renewable resource, they are considered ''green'', a property which is becoming more and more important. Second the pore size of these aerogels is partly in the nanometer-region; therefore they can also be called a nanomaterial.

Lenzing AG, 4860 Lenzing, Austria
E-mail: j.innerlohinger@lenzing.com

Several ways for producing aerogels and aerogel-like materials from cellulosic starting materials (termed aerocellulose in the following) have been investigated. They all follow the well-known aerogel method already introduced by Kistler.[1] First, a wet gel is prepared as a precursor, followed by one or more solvent exchange steps and finally supercritical drying (SC-drying) of the wet gel. Cellulose has to be dissolved[14] for the preparation of the starting gel. In case of the cellulose aerogels this was either done by direct dissolution in caustic soda (NaOH) or *N*-methyl-morpholine-*N*-oxide (NMMO) monohydrate or by using derivatives like cellulose carbamate or cellulose acetate. This work focuses on the preparation of aerocellulose from NMMO solutions, a detailed description for the preparation from cellulose acetate can be found elsewhere.[15] Figure 1 shows the basic scheme for producing aerocellulose from cellulose NMMO solutions. This is a multi step process, where each step influences the following ones and all contribute to the properties of the finally obtained aerocellulose.

Experimental

Materials

Most of the experiments were done with a commercially available eucalyptus pulp, Solucell (Bahia Pulp, Brazil). The other pulps were supplied by the pulp research department of Lenzing AG, see Table 1 for a complete list. The used NMMO (50% in water) was from BASF, Germany. The following solvents were used for the solvent exchange steps: ethanol (absolute, analytical grade; Merck, Germany), methanol (analytical grade; Merck, Germany) and acetone (analytical grade; Merck, Germany).

Sample Preparation

Solution Preparation

NMMO is one of the solvents that can dissolve cellulose directly without prior derivatisation. The region of the water/NMMO/cellulose phase diagram, where complete dissolution is possible, is rather limited.[16] Table 2 summarizes the different concentration ranges used for this study.

The cellulose NMMO solutions were prepared with the help of a laboratory kneader. Ground pulp, NMMO (50–75%) and a stabilizer (gallic acid propyl ester 0.05–0.2%) were placed in the kneader. The pulp was soaked for approximately one hour at reduced pressure and a temperature, which did not exceed 40 °C. Afterwards the temperature was increased and the pressure further reduced in order to remove the excess water from the system. Enough water was removed to shift the concentrations to the region of the phase diagram, where complete cellulose dissolution occurs. Afterwards the pressure was increased again and the solution kneaded for an additional time interval of 15 min. If the pulp was dissolved incompletely the kneading was continued until complete dissolution.

By adding other substances to the cellulose NMMO solution it is possible to obtain composite materials. The system cellulose NMMO offers the possibility to add a variety of substances:

- materials soluble in NMMO[17,18]
- materials, which are molten at the process temperature

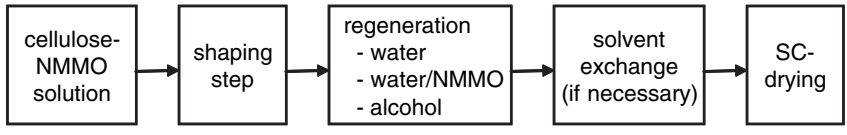

Figure 1.
Schematic representation of the aerocellulose production starting from NMMO/cellulose solutions.

Table 1.
Degree of polymerisation (DP) and kappa number of pulps used in this study, which were investigated regarding their influence on the final product (n. d. = not determined).

Pulp	DP	Kappa number
Eucalyptus pulp "Solucell"	950	0.21
Alkalized Solucell A	535	n. d.
Alkalized Solucell B	207	n. d.
Alkalized Solucell C	198	n. d.
Alkalized Solucell D	179	n. d.
Beech pulp	1486	0.45
Alkalized beech pulp	1181	n. d.
Softwood pulp	2505	n. d.
Paper pulp	4606	0.42
Cotton linters pulp A	950	0.11
Cotton linters pulp B	6292	0.37
Unbleached pulp A	1331	67.8
Unbleached pulp B	3608	20.5

– materials, that can be dispersed in the cellulose NMMO solution

Furthermore the substances should be compatible with the supercritical drying procedure (see below). The initial experiments have been carried out with finely powdered carbon as well as a range of polymers (polyester, polyethylene, and sodium polyacrylate). By choosing the appropriate conditions it is possible to produce all-cellulose composites.[19,20] In our case this has been done by adding short-cut fibres to the cellulose-NMMO solution at the end of the dissolution process.

Shaping of the Cellulose NMMO Solutions

Most of the samples were prepared in monolithic shape by pouring the still hot and liquid cellulose NMMO solution into cylindrical moulds (standard diameter 26 mm). These casts were allowed to solidify at room temperature before further treatment. Small spheres (diameter 2–4 mm) were produced by dripping the molten cellulose NMMO solution through a hole into a regeneration bath (i.e., water) at room temperature or $\sim 0\,^{\circ}C$ (water/ice mixture). These spheres started to regenerate immediately. Even smaller spheres (400–1200 μm diameter) were produced by applying the JetCutter technology[21] by geniaLab (Braunschweig, Germany). This was achieved by cutting a jet of fluid coming out of a nozzle by means of rotating cutting wires into cylindrical segments, which then formed beads due to surface tension on their way to the water bath. Regeneration also started immediately in this case. Another method used was to cast films (with thicknesses from 0.5 to 3 mm) from the cellulose NMMO solutions. These films were either solidified at room temperature before further treatment, or were placed in water while being still partly liquid.

Table 2.
Concentration ranges of the cellulose-NMMO solutions used for this study.

Compound	Concentration [wt%]
Cellulose	0.5–13
NMMO	73–85
Water	13–24

Regeneration and Solvent Exchange

During the regeneration step the cellulose solvent NMMO was replaced with a non-solvent, usually water. As described above, the regeneration of spheres started immediately after shaping, when the cellulose-NMMO solution was still liquid. In contrast, all cylinders were solid before regeneration. All samples were placed in an excess of water, which was stirred and replaced regularly with fresh water until all NMMO had been removed. In a test series, NMMO water mixtures with different NMMO concentrations (20, 25, 40, 50, and 60%) have been used as a first regeneration bath followed by pure water. Ethanol or methanol have been used as alternative regeneration media.

In case of water an additional solvent exchange step had to be performed before SC-drying. Water was replaced either with ethanol followed by acetone or directly with acetone. The solvent exchange was performed the same way as the regeneration: the samples were placed in the corresponding solvent, which was stirred and frequently replaced with fresh solvent until the exchange was completed. For both the regeneration step and the solvent

exchange with different solvents experiments have been performed to determine the corresponding kinetics.[22]

Supercritical Drying

The samples were dried under supercritical conditions, using CO_2 to displace the solvent. The SC-dryings were performed at Natex (Ternitz, Austria) with a 5 Liter/1000 bar plant or a smaller 200 ml laboratory facility. Most of the samples were dried from acetone, and a few were dried from ethanol and methanol for comparison.

The wet gels were placed in a high-pressure vessel, which was filled with additional solvent in order to prevent a premature drying of the samples by solvent evaporation. The vessel was closed and heated slowly according to a given temperature ramp. Then liquid CO_2 (at about 60 bar) from a storage tank was pressurized to 90 to 200 bar and heated up to 40 °C before entering into the extractor. After the drying conditions were reached the samples remained in the extractor without CO_2-flow. The supercritical CO_2 was able to penetrate into the samples to form a homogeneous mixture with the organic solvent inside and outside the sample. Then the CO_2 flow started and diluted the organic solvent CO_2-mixture. The solvent-loaded CO_2 was depressurized into a second vessel in order to separate the organic solvent from the gaseous CO_2. CO_2-flow was maintained until the organic solvent was completely removed from the samples. In the final step the vessel was depressurized to atmospheric pressure according to a certain pressure-time gradient and the dried samples were unloaded.

Analytical Methods

N_2-adsorption and desorption were measured at 77 K with a Belsorp mini II (Bel Inc, Japan) after vacuum pre-treatment of the samples for 6 h. From the isotherms the BET-surface[23] and the BJH-pore size distribution[24] were calculated. Electron micrographs of selected samples were prepared by a Hitachi S-4000 SEM (Hitachi, Japan) with an acceleration voltage of 5 kV after 60 sec metallisation with Au/Pd. The bulk density of the cylindrical samples was determined by simply weighing, and measuring their size. To have at least some characterisation of the wet gels, their size was measured throughout the process to determine the shrinkage.

Results and Discussion

The most crucial step in producing cellulose aerogels is the drying procedure to get dry aerogels from the wet gel precursors. If the wet gels are dried at ambient conditions the strong capillary forces will cause the porous structure to collapse and as a consequence destroy the high internal surface area. To prevent this, a more sophisticated method of drying the acetone or alcohol gels is needed. The aerogels described in this work were dried with CO_2 under supercritical conditions, where no capillary forces are present. If polymeric additives are used in the samples, they have to be compatible with the SC-drying process. It is known that the melting point of polymers can be reduced in the presence of compressed gases.[25] There is the potential that the polymeric additives can be removed from the cellulosic gel in this way, and block valves or pipelines.

Once successfully produced the characterisation of the highly porous aerocellulose is no trivial problem[26] as the ultrastructure can already be altered or even destroyed by the measurement. One of the more reliable methods is the measurement of nitrogen adsorption,[27] which was the analytical tool used for most of the dried samples. To get a detailed picture of the influence of the various production parameters of all steps an analysis of the wet gels would also be needed. Unfortunately the available methods are rather limited. Small angle X-ray scattering (SAXS) is a possible method to investigate the pore structure of such wet gels.[28] Some preliminary SAXS-experiments showed the applicability of the method for the hydro- and alcogels used in this study. However, more experiments will

be needed to adapt the method to these samples.

Despite the described limitations and the fact that we were dealing with a completely new material the obtained results are more than satisfactory. More than 300 different samples were prepared and analysed. More than 300 samples with densities in a range from 0.014 g/cm^3 to 0.5 g/cm^3 and internal surface areas ranging from 50 m^2/g to 420 m^2/g were produced from the different starting materials described above.

The volume loss throughout the whole production from the solid cellulose- NMMO casts to the final light-weight aerocellulose can be quite high, reaching as high as 90%. Figure 2 shows the remaining volume of the cylinders after regeneration, solvent exchange and SC-drying, depending on the initial cellulose concentration. The standard deviation is rather high as the samples are grouped by their initial cellulose concentration while other production parameters were not constant. For samples produced using the same set of parameters the standard deviation for the volume loss is below 5%. The density shows a similar standard deviation and the repeatability for the internal surface area is even better.

It can be seen in Figure 2 that the shrinkage decreases with increasing initial cellulose concentration and then reaches a plateau. The density shows a similar dependence on the initial cellulose concentration, shown in Figure 3. As expected, the density increases with increasing cellulose concentration. The samples with 5 wt% cellulose show a higher density than it would be expected from the trend of the other data. It should be noted that only five cylinders contributed to this value and that they were all in the same batch during SC-drying. The corresponding shrinkage during this step was high and the remaining volume is rather low (see Figure 2). This leads to the conclusion that there was some kind of error during this drying run.

As mentioned above, the SC-drying step greatly influences the properties of the aerocellulose. Imperfect drying usually leads to higher shrinkage of the samples in this step, resulting in bodies with a higher density and with a decreased internal surface area. During some drying trials, the pore structure of the samples collapsed

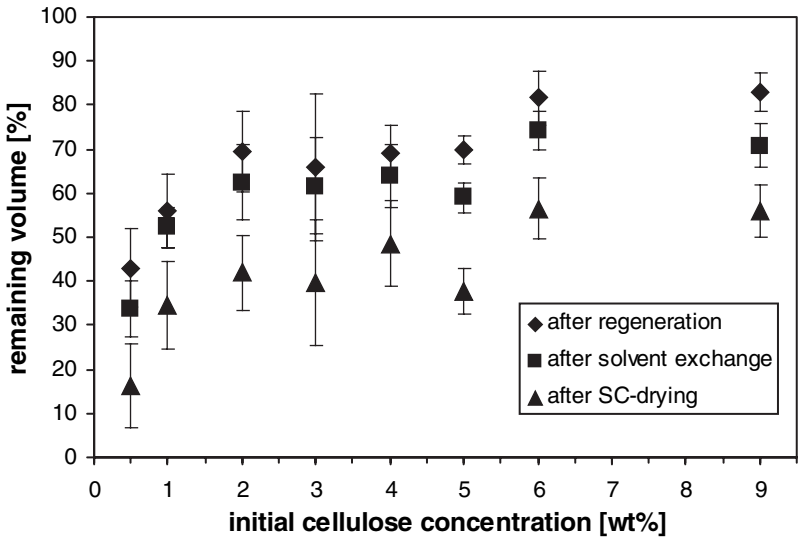

Figure 2.
Average remaining volume (and standard deviation thereof) of the cylinders depending on the initial cellulose concentration.

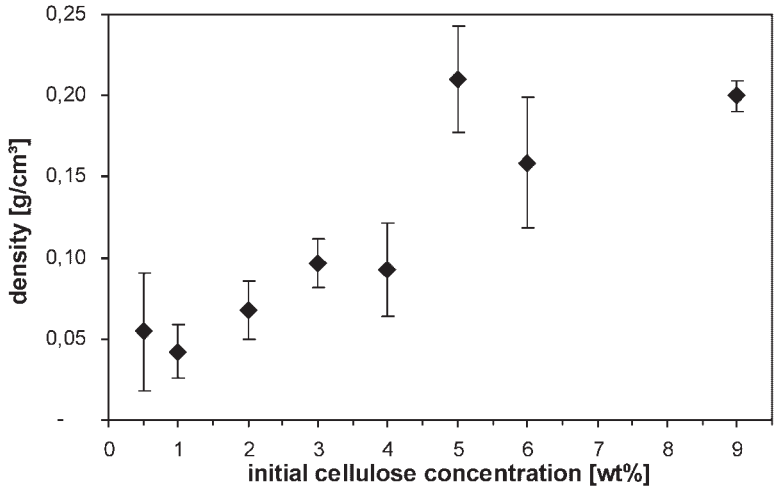

Figure 3.
Average density (and standard deviation thereof) of the aerocellulose cylinders after SC-drying in relation to the initial cellulose concentration.

nearly completely. The samples seem to be very sensitive to an abrupt temperature rise before reaching supercritical conditions inside the vessel. Also a small amount of residual solvent from the production chain, such as NMMO or water, can downgrade the result of the SC-drying. On the one hand, the SC-drying is very sensitive to some parameters like those just described, but is also very robust with respect to other parameters. In two cases the SC-drying had to be aborted during the procedure and the samples were still acetone-wet after opening the vessel. After a second successful drying the properties of the samples were not inferior compared to the average. Table 3 shows the influence of the SC-drying procedure on shrinkage, density and internal surface area. Cylinders (2.28 wt% Solucell) from the same preparation were added to different SC-drying batches. During the regeneration and the solvent exchange these cylinders showed the same shrinking behaviour. The results from drying trial no. 4 are clearly below average, although no irregularities were observed during this run. In contrast trial no. 5 was one of the ''double'' dryings described above, but the obtained internal surface area is clearly above the average despite of the rather high shrinkage during drying.

Figures 2 and 3 show the correlations between the initial cellulose concentration and shrinkage/density. The trend is as expected: a higher initial concentration of

Table 3.
Comparison of different supercritical (SC) drying trials regarding the properties of the obtained aerocellulose (* ''double'' drying).

SC drying trial-nr.	Density [g/cm³]	$a_{S,BET}$ [m²/g]	Shrinkage during SC-drying [%]	Total remaining volume [%]
1	0.085	188.1	41	36
2	0.082	187.1	39	38
3	0.088	179.3	45	34
4	0.098	169.4	55	29
5*	0.083	208.1	50	31
6	0.082	193.1	52	31
7	0.067	193.2	36	40
8	0.069	208.9	37	40

cellulose yields bodies with a higher density and with less shrinkage. A similar behaviour was expected for the internal surface area: more cellulose should result in a smaller internal surface area. However, the data showed that these two parameters are not correlated. Also no influence of the DP of the used pulp on the obtained BET-surface can be found. Although the DP has no influence, a correlation of the used pulp type with the final density was observed when using unbleached pulp. The two unbleached pulps with a higher lignin-content resulted in cylinders with a density of 0.036 ± 0.011 g/cm^3 compared to 0.081 ± 0.009 g/cm^3 for Solucell. The initial cellulose concentration of the compared samples was ~2 wt% in all cases. The lower density may be due to lignin still present in the pulps, but no further investigation of this phenomenon exists so far.

It is difficult to establish correlations like the one described above between the production parameters and the properties of the final product. Many samples were prepared and analysed in order to have a sufficient data pool. Although more than 300 different samples have been prepared, only a small data set is available for some parameters. That is because the whole production chain is rather long and a detailed analysis is only possible for the final products, but not for the intermediates. However, some clear relationships were found which were not obvious from the beginning.

It was found that some modifications of the regeneration/solvent exchange chain have a significant, reproducible influence on the final properties while others do not (at least with the limited data of this study). Statistical significant differences were investigated with a simple one factorial variance analysis (ANOVA) using a confidence interval $\alpha = 0.05$. There is no observable difference between regeneration in water, ethanol or methanol as long as all NMMO is removed. The samples regenerated in ethanol or in methanol were directly SC-dried from these solvents, or in some cases exchanged with acetone and then dried. Water regenerated samples were exchanged with ethanol followed by acetone, or directly with acetone before SC-drying. All the described procedures resulted in approximately the same shrinkage, the same density and the same internal surface area when comparable cellulose concentrations were used. The only regeneration bath which showed an influence on the final aerocellulose was the NMMO-water mixture. When an NMMO-water mixture was used as a first regeneration bath, the internal surface area of the resulting aerocellulose was lower than for the other procedures. This behaviour was observed for both cylinders and spheres. Figure 4 shows the internal surface areas of different samples obtained from Solucell solutions with an initial concentration of ~2 wt%. Beside the already described influence of NMMO-water mixtures as regeneration bath, the other significant difference is between cylinders and spheres. The spheres show a higher internal surface area compared to the cast cylinders. An especially high internal surface area was achieved by dripping the cellulose-NMMO solution into an ice/water bath instead of water at ambient temperature. The rest of the production chain was identical: regeneration in water, solvent exchange to acetone and SC-drying. The obtained aerocellulose spheres were also different macroscopically. While the spheres from ice/water were completely solid, the spheres formed at room temperature showed a dense skin and a rather fluffy core. A similar behaviour was observed for the films. When they were solidified before regeneration, the obtained samples were homogenously solid, whereas starting the regeneration with the still partly liquid films resulted in some kind of "hollow" films.

As the BJH theory assumes cylindrical pores, it can only be used as a rough estimate for the rather complex pore structure of the aerocellulose (see electron micrographs in Figures 5 and 6). For most samples the number of pores increases from 100 nm down to 1 nm in the BJH-plots. It was found that many of the samples with a

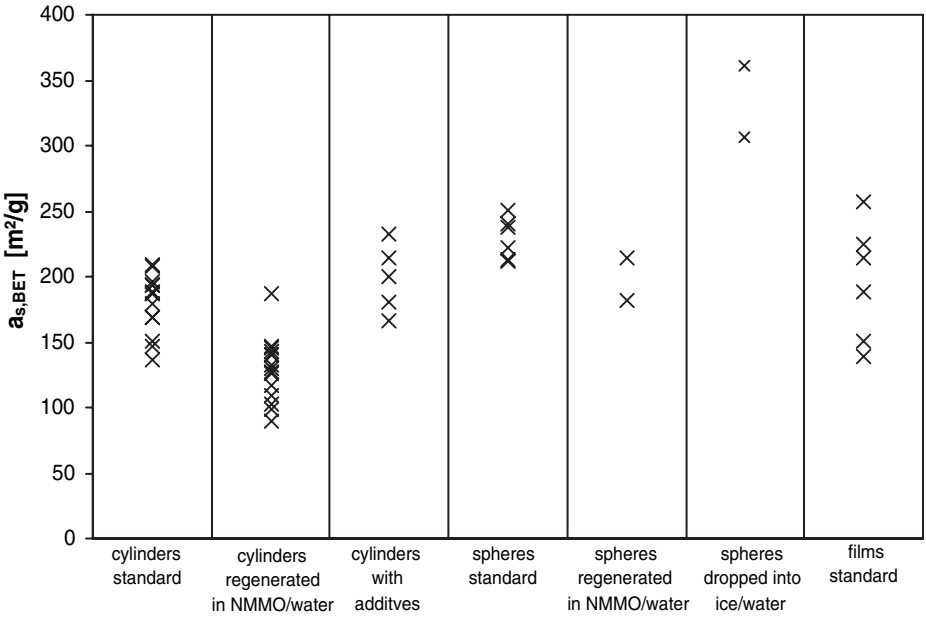

Figure 4.
BET surfaces of different samples from ~2% Solucell solutions. Statistical significant differences (ANOVA, $\alpha = 0.05$) between standard cylinders and such ones regenerated in NMMO and between standard cylinders and spheres. No significant difference between standard cylinders, cylinders with additives and standard films.

high BET-surface show a peak in the BJH-plot around 10 nm. The relation between production parameters and the BJH pore size distribution has not been analysed in detail.

The BJH-plots give a hint about the pores in the 1–100 nm regime. To get a picture of the pore structure in the μm range, SEM images of selected samples have been made. Figure 5 shows some of the typical structures, which can be found inside and on the surface of the aerocellulose samples. The depicted network- or sponge-like porous structure can be found in nearly all samples regardless of their origin. Sometimes fibre-like structures or congregations of small granules can be found embedded in the network. The surface of the samples is relatively smooth and consists of a more compact structure. Cracks and gaps allow a look at the network structure, which is already beginning just below the surface.

Samples with a reduced internal surface area due to a (partial) collapse of the porous structure during SC-drying show a different morphology (Figure 6). The finely divided network is gone, resulting in a more dense structure, which consists of plates and resembles a honeycomb. The results from the shrinkage, the density, the BET surface and the electron micrographs are consistent for all these samples. The collapsed samples have a higher shrinkage and a much lower internal surface area compared to the intact ones. They are also denser – as expected.

Conclusion

The rather simple methods of measuring the size and density of the samples, in connection with the more sophisticated methods of nitrogen adsorption and electron microscopy, allow a good characterization of the aerocellulose samples for relation to their production conditions. For an even more detailed picture, additional methods like SAXS would be desirable. From all the data gathered, possible ways of

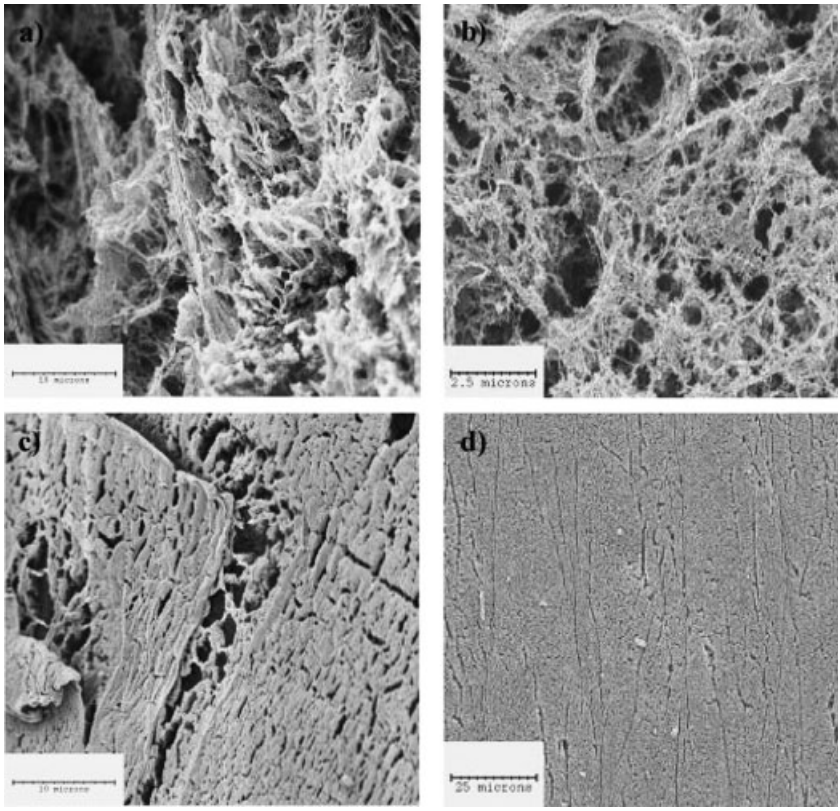

Figure 5.
SEM images of typical aerocellulose structures. a) Interior of a cylinder (scale bar 10 μm). b) Interior of a film (scale bar 2.5 μm). c) Surface of a sphere produced with the JetCutter (scale bar 10 μm). d) Surface of a film (scale bar 25 μm).

manipulating the properties of the product aerocellulose have been extracted. Some of them are rather obvious, like increasing the density by adding more cellulose to the solution at the beginning. The control of the internal surface area (and structure) is more complicated as it does not depend on the initial cellulose concentration or the

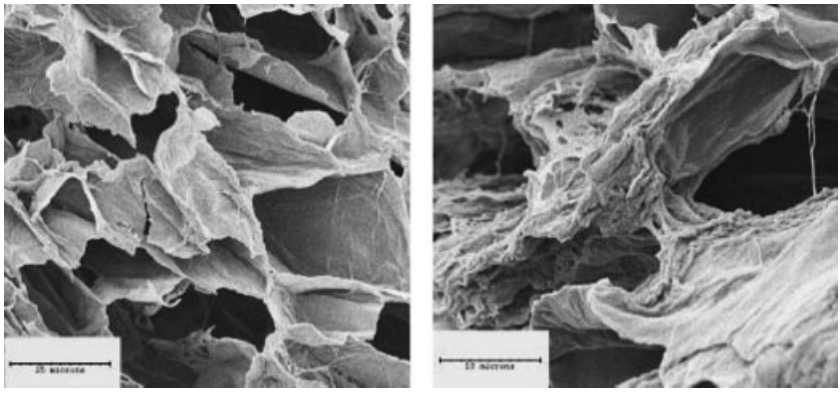

Figure 6.
Internal structure of samples partly collapsed during the SC-drying process (scale bars 10 μm).

nature of the pulp used. The internal surface area can be influenced by choosing the appropriate regeneration conditions or by deliberately worsening the results of the SC-drying if a lower surface is needed.

Properties such as high internal surface area and low density together with others like mechanical stability, insulation properties and biodegradability make aerocellulose an ideal candidate for various applications. Initial application tests at laboratory scale show promising results. Some of the organic aerogels have been pyrolysed to carbon aerogels, which have been tested in selected electrochemical applications.

Altogether the knowledge gained about cellulose aerogels during the AeroCell project is quite formidable and already the first application tests show the great potential of this class of materials. Nevertheless, more research and a deeper understanding of these complex systems are needed before a possible commercialisation.

Acknowledgements: The authors thank all the partners for the good cooperation and fruitful discussions. Preparation of the small spheres via JetCutter was done at geniaLab by S. Siebenhaar and SC-drying was performed at Natex with help of E. Lack, M. Sova, and F. Lang jun. We thank G. Kandioller (WOOD Analytikzentrum Lenzing) for providing the SEM images. Financial supported was granted by the EC 6th framework program, contract number NMP3-CT2003-505888 (project acronym: AeroCell).

[1] S. S. Kistler, *J. Phys. Chem.* **1932**, *36*, 52.
[2] S. S. Kistler, *Nature* **1931**, *127*, 741.
[3] M. Schmidt, F. Schwertfeger, *J. Non-Cryst. Solids* **1998**, *225*, 364.
[4] V. Bock, A. Emmerling, R. Saliger, J. Fricke, *J. Porous Mater.* **1997**, *4*, 287.
[5] R. W. Pekala, *J. Mater. Sci.* **1989**, *24*, 3221.
[6] D. W. Schaefer, R. Pekala, G. Beaucage, *J. Non-Cryst. Solids* **1995**, *186*, 159.
[7] J. Yamashita, T. Ojima, M. Shioya, H. Hatori, Y. Yamada, *Carbon* **2003**, *41*, 285.
[8] C. Moreno-Castilla, F. J. Maldonado-Hódar, *Carbon* **2005**, *43*, 455.
[9] H. Jin, Y. Nishiyama, M. Wada, S. Kuga, *Colloids and Surfaces A: Physiochem. Eng. Aspects* **2004**, *240*, 63.
[10] C. Tan, B. M. Fung, J. K. Newman, C. Vu, *Adv. Mater.* **2001**, *13*, 644.
[11] R. C. Weatherwax, D. F. Caulfield, *Tappi* **1971**, *54*, 985.
[12] J. Innerlohinger, H. K. Weber, G. Kraft, *Lenzinger Ber.* **2006**, *86*, 137.
[13] F. Fischer, E. Guilminot, M. Chatenet, A. Rigacci, S. Berthon-Fabry, E. Chainet, P. Achard, "Nanostructured carbons from cellulose aerogels for PEM-FC electrodes: elaboration and electrochemical characterization"; *7th European Symposium on Electrochemical Engineering* **2005**, Toulouse, France.
[14] T. Heinze, A. Koschella, *Polimeros: Ciencia e Tecnologia* **2005**, *15*, 84.
[15] F. Fischer, A. Rigacci, R. Pirard, S. Berthon-Fabry, P. Achard, *Polymer* **2006**, *47*, 7636.
[16] R. N. Armstrong, C. C. McCorsley, J. K. Varga, "Spinnable solutions of cellulose in amine oxides"; *5th International Dissolving Pulps Conference* **1980**, Atlanta, USA.
[17] N. Nagashima, S. Matsuzawa, M. Okazi, *J. Appl. Polymer Sci.* **1996**, *62*, 1551.
[18] Y. Xu, Y. Zhang, H. Shao, X. Hu, *Int. J. Biol. Macromol.* **2005**, *35*, 155.
[19] W. Gindl, J. Keckes, *Polymer* **2005**, *46*, 10221.
[20] T. Nishino, I. Matsuda, K. Hirao, *Macromolecules* **2004**, *37*, 7683.
[21] U. Prüße, J. Dalluhn, J. Breford, K.-D. Vorlop, *Chem. Ing. Tech.* **2000**, *72*, 852.
[22] G. Kraft, *in preparation.*
[23] S. Brunauer, P. H. Emmet, E. Teller, *J. Amer. Chem. Soc.* **1938**, *60*, 309.
[24] E. P. Barrett, L. G. Joyner, P. P. Halenda, *J. Amer. Chem. Soc.* **1951**, *73*, 373.
[25] E. Weidner, V. Wiesmet, Z. Knez, M. Skerget, *J. Supercrit. Fluids* **1997**, *10*, 139.
[26] G. W. Scherer, *Adv. Colloid Interface Sci.* **1998**, *76–77*, 321.
[27] K. Sing, *Colloids and Surfaces A: Physiochem. Eng. Aspects* **2001**, *187–188*, 3.
[28] H. Ando, T. Konishi, *Phys. Rev. E* **2000**, *62*, 727.

